

Research Article

Comparison of Output Performance of Tunable Lasers with Two Different External Cavities

Ya Wang , Shengbao Zhan , Wenran Le , Qinghai Liu , Yuting Wang , Lin Zou ,
and Zhifeng Deng 

School of Electronic Engineering and Intelligent Manufacturing, Anqing Normal University, Anqing, Anhui 246133, China

Correspondence should be addressed to Shengbao Zhan; zhanshb@aliyun.com

Received 20 May 2022; Revised 14 July 2022; Accepted 22 July 2022; Published 17 August 2022

Academic Editor: Sulaiman W. Harun

Copyright © 2022 Ya Wang et al. This is an open access article distributed under the Creative Commons Attribution License, which permits unrestricted use, distribution, and reproduction in any medium, provided the original work is properly cited.

Based on the simplified model of the tunable fiber laser system, the tuning performance of the laser was analyzed. Two kinds of tunable setups were established, which are the configurations with an external cavity and the configuration of the Littrow cavity. The tuning output characteristics experimentally were analyzed by means of setups. The simulation gives the output efficiency of two tunable lasers as 40% and 30%. In the experiment, the measured slope efficiency of the two lasers was 24% and 18.3%, and the tunable range of the two lasers was 32 nm and 40 nm, respectively. Both lasers could achieve laser output with good beam quality.

1. Introduction

The fiber laser is widely used in many fields, including optical communication, industrial manufacturing, and fiber sensing systems [1–4], which require that the output beam of the laser can be tuned to one or more specific wavelengths. Therefore, tunable fiber lasers have become important optical devices. A tunable external cavity fiber laser can achieve tunable wavelengths by tuning the optical element [5, 6]. Various external cavity tunable fiber lasers system with the grating have been reported, which include the configuration with an output coupled mirror in an external cavity (the laser is called configuration); and the configuration with a Littrow cavity (the laser is called configuration); the maximum continuous tunable range can be up to several tens of nanometers; and the linewidth of the output beam is effectively narrowed [7–11]. However, when we compare the external cavity tunable lasers with different configurations, the output performances of lasers are different. Most researchers only reported their experimental results in tunable lasers but did not carry out a theoretical and experimental comparison of the performance between the different external cavity tunable lasers.

In this study, two kinds of tunable lasers with different external cavity configurations are studied. First, the output

effect of the two lasers is analyzed theoretically. Then, using a diffraction grating with a diffraction efficiency of 70% as a wavelength selector, we build two experimental systems of the external cavity tunable fiber lasers and compare their experimental results. The results show that configuration 1 can realize the tunable range of 32 nm with the maximum output power of 560 mW and for configuration 2, can achieve the maximum output power of 427 mW with the tunable range of 40 nm. Both two tunable fiber lasers can produce single-mode output with a beam quality factor (M^2) < 1.35.

2. Theoretical Analysis

2.1. Simplification of Tunable Systems. Figures 1(a) and 1(b) show the schematic diagram of configurations 1 and 2, respectively. According to the generation principle of laser, the system can be simplified, as shown in Figure 2 [12].

In Figure 2, the inserted devices in configuration 1 are the collimating lens and grating and those in configuration 2 are the collimating lens and DM2. Assuming the length of the gain fiber is L , that of the resonator is L' , launched pump power is P_p^{in} , and the output power is P^{out} . According to the framework shown in Figure 2, if the transmissivity of the

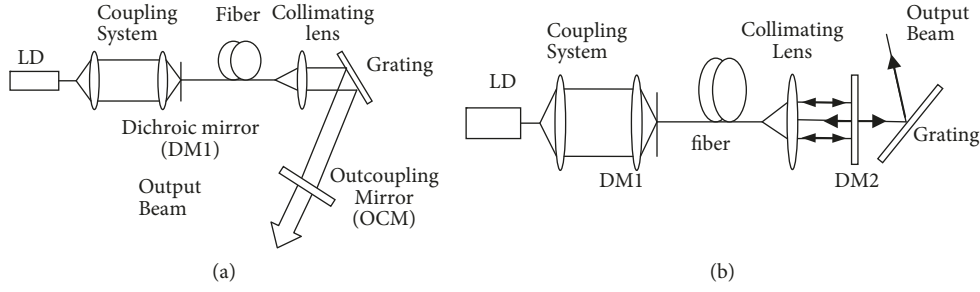


FIGURE 1: Schematic diagram of tunable fiber laser (a). Configuration 1 (b). Configuration 2.

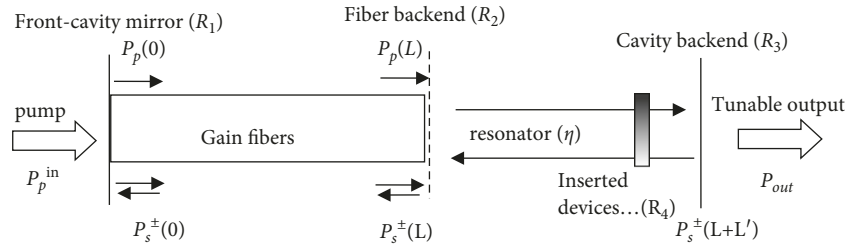


FIGURE 2: The framework of a simplified tunable fiber laser system.

front-cavity mirror to the pump light equals 1, then the following equations can be obtained [12]:

$$\begin{aligned}
 P_p(0) &= P_p^{\text{in}}, \\
 P_s^+(0) &= R_1 P_s^-(0), \\
 P_s^-(L) &= R_2 P_s^+(L) + (1 - R_2)^2 (1 - R_4)^2 \eta(\lambda) R_3 K(\lambda) P_s^+(L), \\
 P^{\text{out}} &= P_s^+(L) (1 - R_2) (1 - R_3) (1 - R_4) K(\lambda),
 \end{aligned} \tag{1}$$

where $K(\lambda)$ is the diffraction efficiency of a blazed grating, and $\eta(\lambda)$ is the coupling efficiency that the signal light is coupled back into the fiber core.

For $K(\lambda)$, it can be derived as

$$K(\lambda) = K_0 \sin^2 c^2 \left\{ \frac{bm}{d} - b \tan \theta \frac{\cos[\sin^{-1} m(\lambda_c - \lambda_j)/d] + \cos[\sin^{-1} m\lambda_c/d]}{\lambda_j} \right\}, \tag{2}$$

where K_0 is a constant with respect to the grating structure, d is the grating period, b is the lateral size of the diffractive facet, m is the diffraction order, and θ is the blazed angle.

If $d = 2.43 \mu\text{m}$, $b = 5 \mu\text{m}$, $\lambda_c = 1550 \text{ nm}$, $K_0 = 0.70$, and $m = 1$, the diffraction efficiency of the grating at different wavelengths could be obtained, as shown in Figure 3. It can be seen that the diffraction efficiency of the grating gradually increases from 1500 nm to 1545 nm, the diffraction efficiency gradually decreases from 1545 nm to 1600 nm, the highest diffraction efficiency is 0.70 at 1545 nm, and the lower diffraction efficiency is 0.598 at 1600 nm.

In the tuning performance analysis, another parameter of η must be used. For the parameter, Bochove has carried out the derivation [9], which can be written as

$$\eta(\lambda) = \frac{\exp[-4(\theta_x^2 + \theta_y^2)/\theta_0^2] \exp[-(\lambda - \lambda_0)^2/\sigma^2]}{\sqrt{(1 + \omega_x^2)(1 + \omega_y^2)}} K^2(\lambda), \tag{3}$$

where $\theta_0 = \lambda/\pi w_0$ is the far-field divergence angle of the Gaussian mode field, σ is the coupling bandwidth, and ω_x and ω_y are the wavefront curvature parameters, which are [13]

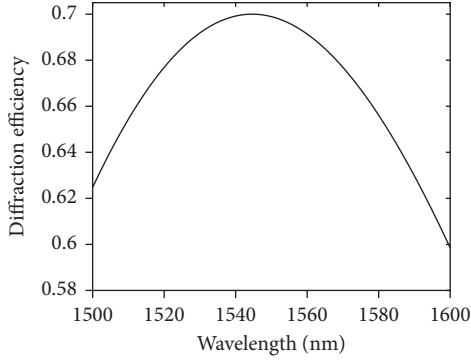


FIGURE 3: Diffraction efficiency as a function of wavelength.

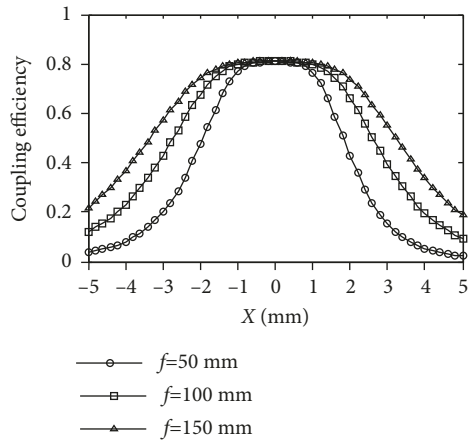


FIGURE 4: The coupling efficiency versus transverse distance and lens focal length.

$$\omega_x = \frac{\varepsilon}{Z_R} + \frac{\alpha X^2 + \beta Y^2}{f Z_R}, \quad (4)$$

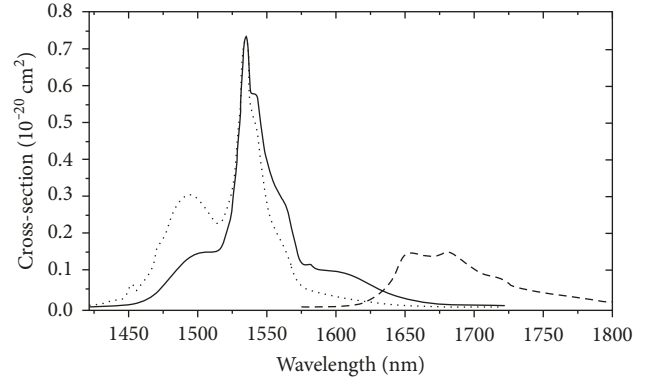
$$\omega_y = \frac{\varepsilon}{Z_R} + \frac{\beta X^2 + \alpha Y^2}{f Z_R},$$

where Z_R is the Rayleigh length of the mode field, ε is a defocus value, X is the transverse distance of the emitter from the system axis, Y is the emitter lateral offset out of the array plane, α and β are the parameters determined by transform lens, $\alpha = 3$ and $\beta = 1.33$ [13].

If $Y = 0$, $\theta_{x,y} = 0$, and $\varepsilon = 0$, for different focal lengths of transformed lenses, the coupling efficiency at different transverse distances from the system axis can be obtained according to Equation (3), as shown in Figure 4. It can be seen that when the transverse distance increases, the coupling efficiency of the laser decreases gradually, and the coupling efficiency gradually increases with the increase of the focal length of the transform lens.

2.2. Analysis of Tuning Performance

2.2.1. Relevant Parameters. In the theoretical analysis, if the used gain fiber is $\text{Er}^{3+}/\text{Yb}^{3+}$ codoped double-clad fiber with a fiber length of 4 m. The relevant parameters include the



— Er^{3+} Emission
 ···· Er^{3+} Absorption
 --- Er^{3+} ESA

FIGURE 5: Er^{3+} absorption-emission cross-sections.

TABLE 1: Relevant simulation parameters.

Parameters	Values
R_2	4%
R_4	5%
K_0	0.7
Focal length f	50 mm
Mode field radius w_0	10 μm
Grating period	2.43 μm
Central wavelength λ_c	1550 nm
Pump power P_p	2 W

spectrum absorption-emission cross-sections (σ_{Era} and σ_{Ere}) of Er^{3+} , as shown in Figure 5 [14].

According to the parameters of the fiber given by the Nufern Company, the core diameter of the fiber is 25 μm , the clad diameter is 300 μm , and the coating diameter is 450 μm . In addition, the concentration of Er^{3+} and Yb^{3+} doped in the fiber is $4.8 \times 10^{25} \text{ m}^{-3}$ and $3.7 \times 10^{26} \text{ m}^{-3}$, respectively, and the lifetime of Er^{3+} is $11 \times 10^{-3} \text{ s}$. Assuming the wavelength of the pump is 980 nm, the transition cross-sections $\sigma_{\text{Er}13} = 2.0 \times 10^{-25} \text{ m}^2$ and $\sigma_{\text{Yb}65} = 5.0 \times 10^{-25} \text{ m}^2$. Other relevant parameters involved are given in Table 1 [15, 16].

2.2.2. Simulation Results. Assuming the tunable range is 1500–1600 nm, the tuning step is 5 nm, $Y = 0$, $\theta_{x,y} = 0$, $\varepsilon = 0$, and $R_1 = 0.90$, and the power of the tuning laser at different wavelengths was calculated, as shown in Figure 6.

For configuration 1, maximum output power is 800 mW, at a wavelength of 1547 nm, the minimum power is 210 mW at 1600 nm, and the calculated maximum output efficiency is 40%. Furthermore, the laser output power increases gradually in the range of 1500–1547 nm, and the output power gradually decreases in the range of 1547–1600 nm. For configuration 2, the maximum power is 600 mW at 1555 nm, the minimum power is 345 mW at 1500 nm, and the maximum output efficiency is 30%.

The output power of the laser changes greatly at different wavelengths. The reason is that the diffraction efficiency of

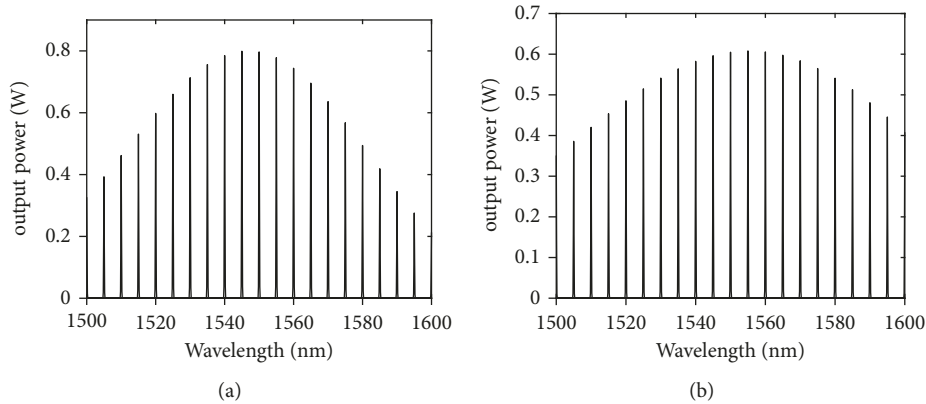


FIGURE 6: Change of output power with wavelength. (a) Configuration 1. (b) Configuration 2.

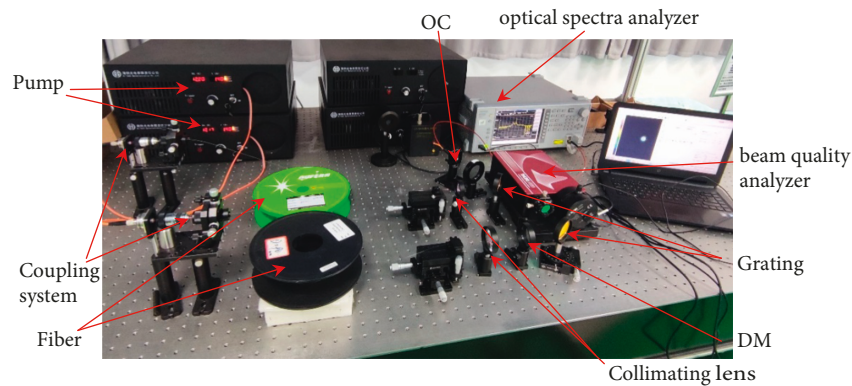


FIGURE 7: Experimental setup for producing tunable laser.

the grating at different wavelengths is different, and the absorption-emission cross-section of the optical fiber at different wavelengths is different. The difference in output efficiency between the two configurations is mainly caused by the difference in feedback intensity (R_3) at the backend of the external cavity. As the increase of the backend feedback intensity, the output efficiency gradually decreases [12].

3. Experiment

3.1. Experimental Setup. In two kinds of laser configurations, the pump was provided by a laser diode with a central wavelength of 976 nm through a coupled system. The maximum power coupled into the fiber was 3.0 W. The fiber used was LMA $\text{Er}^{3+}/\text{Yb}^{3+}$ codoped double-clad fiber named PLMA-EYDF-25P/300-HE with a length of 4 m, whose core had a diameter of 25 μm with a numerical aperture (NA) of 0.09. The absorption coefficient was 2.9 dB/m at 980 nm. A dichroic mirror (DM1, high transmission to pump, and high reflectivity to signal light) was placed at the input end of the fiber, which served as the front-cavity mirror of the resonator. The output end of the fiber was angle cleaved to suppress Fresnel reflection. A collimating lens ($f=50$ mm) was placed at the output end of the fiber. The experimental setups are shown in Figure 7.

For configuration 1, the first-order diffracted beam of the grating was incident on the outcoupling mirror (OCM),

which has a reflectivity of 15% to provide feedback for laser oscillating and achieve laser output. For configuration 2, to improve the conversion efficiency and output power of the fiber laser, DM2 (high transmission to signal light and high reflectivity to pump) is placed behind the collimating lens. The grating was placed according to the Littrow angle, the first-order diffracted beam was reflected back, and the zeroth-order diffracted beam was used as the output beam.

In addition, the grating has a frequency of 1200 lines/mm with a blazing wavelength of 1550 nm, and the first-order diffraction efficiency of the grating can reach 70%. The laser beam quality was measured using a beam quality analyzer (M2MS BP209-IR), and the spectral performance was analyzed by an optical spectra analyzer (model: MS9710B).

3.2. Comparison of Experimental Results

3.2.1. Comparison of Tunable Ranges. First, using configuration 1, the experiment was carried out. When the coupled pump power was 3 W, the tuned laser at the range of 32 nm from 1532 nm to 1564 nm was achieved, as shown in Figure 8(a). For each spectrum of the tuned laser, the measured 3 dB linewidth was less than 0.08 nm. The suppression of the ASE background was better than 46 dB. Next, the experiment of configuration 2 was conducted, as shown in Figure 8(b). At the coupled pump power of 3 W, the

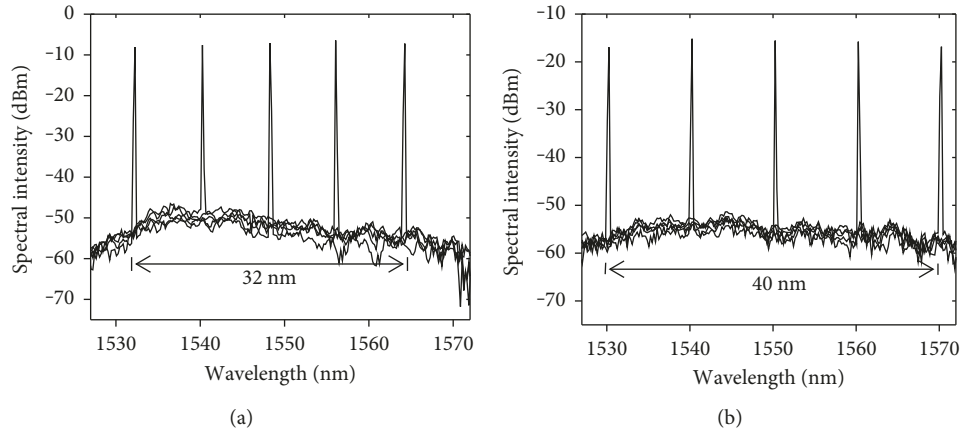


FIGURE 8: Tunable output laser spectra. (a) Configuration 1. (b) Configuration 2.

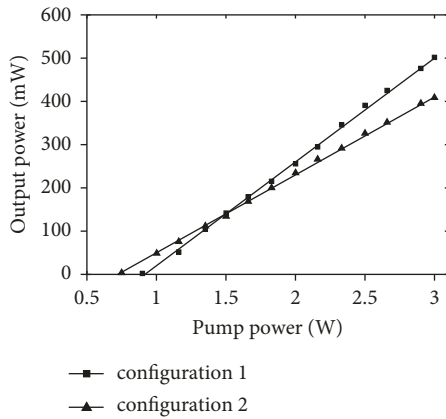


FIGURE 9: The slope efficiency when the tuning wavelength is 1546 nm for configuration 1 and 1550 nm for configuration 2.

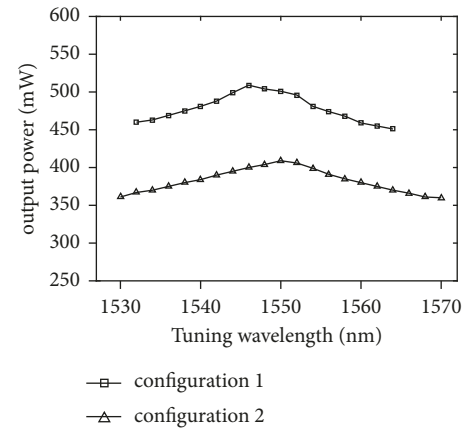


FIGURE 10: Tuning power versus wavelength.

measured maximum tuning range is 40 nm from 1530 nm to 1570 nm. For each spectrum of the tuned laser, the measured 3 dB linewidth was less than 0.1 nm. The suppression of the ASE background was better than 41 dB.

Compared to Figures 8(a) and 8(b), the tunable range of configuration 2 is wider than that of configuration 1. This is because the backend of the external cavity of configuration 1 is OCM, which has low feedback for the signal light. According to the curve in Figure 6, for configuration 1, the weak feedback signal light cannot induce a more population of Er^{3+} transitions. For configuration 2, the backend of the external cavity is the grating, which has higher feedback for the signal light, and the higher feedback intensity can induce more population of Er^{3+} to finish the energy level transition, realizing the tuned laser output in a wider band.

Furthermore, we also compared the tuning range of the simulation and the experiment. It can be found that the tuning range in the experiment is narrower than that in simulation. This is because the oscillation threshold of two configurations is different at different wavelengths; it can also be found in Figure 9 (Section 3.2.2). However, the oscillation threshold is set to a small constant in the simulation, which makes laser oscillation be produced at lower power, resulting in a wider tuning range.

3.2.2. Comparison of Output Power. In the experiment, the measurements of the laser output power of the two configurations at different coupled pump power were made, as shown in Figure 9. When the coupled pump power was 3 W, the maximum laser output of 501 mW at 1546 nm was achieved by configuration 1 with a slope efficiency of 24%. For configuration 2, the maximum output power is 409 mW at 1550 nm with a slope efficiency of 18.3%. The output efficiency of the tuned output laser in the experiment is lower than that in the simulation. This is because the angle-cleaved facet of the fiber is not polished, and the lenses used in this experiment do not have an antireflection coating of a 1550 nm band, which reduces the efficiency of the lasers. In addition, with the increase of the pump power, the output laser power increases approximately linearly, and saturation gain does not occur, which means that the pump power can be continuously increased to obtain higher output power.

Furthermore, the output power of the tunable laser at different wavelengths is measured, which is shown in Figure 10. It can be seen that the wavelength of maximum power in the experiment is slightly different from that in the calculation because of the different lengths of the resonators. The output power of configuration 1 is higher than that of configuration 2; this is because considering all external

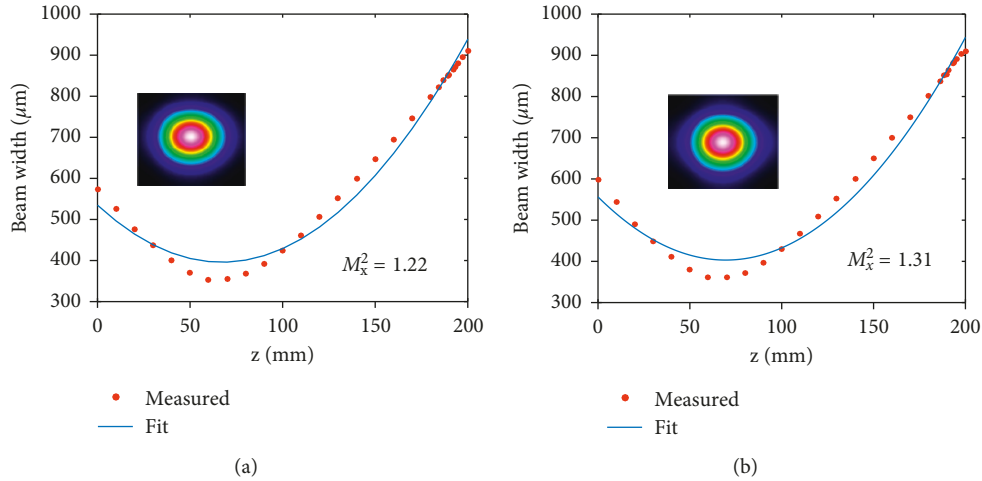


FIGURE 11: Beam quality of the tuning laser at 1548 nm. (a) Configuration 1. (b) Configuration 2.

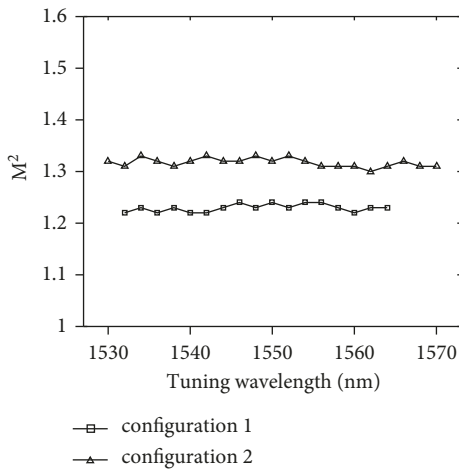


FIGURE 12: Wavelength verse beam quality.

cavity loss factors, the total feedback level of first-order diffraction light is over 50% in configuration 2, and the grating diffraction efficiency of zero-order light is 25%, which lead to a lower outcoupling ratio of the resonator, and cause large cavity loss and limit the effective increase of the output power and slope efficiency of the tunable fiber laser. However, in configuration 1, the feedback intensity of the external cavity is about 15%, which causes a higher outcoupling ratio and increases the efficiency of the resonator. Furthermore, the slope efficiency and output power of the laser can be improved by reducing the external cavity loss and adopting the backward output configuration [15].

3.2.3. Comparison of Beam Quality. When the wavelength of the output laser was 1548 nm, the output beam quality factor (M^2) of the two lasers was measured, as shown in Figure 11. For configuration 1, the measured M_x^2 is 1.22, and for configuration 2, $M_x^2 = 1.31$. Compared with the ideal Gaussian beam, the beam quality is degraded; this is due to the aberration of the transform lens and the etching error of the grating.

Figure 12 shows the measurement results of the M^2 in the tuning range. The M^2 of configuration 1 is kept at the range of 1.22–1.26, and M^2 of the configuration 2 is kept in the range of 1.31–1.34. The output beam quality of configuration 1 is better than that of configuration 2; the reason is that the direction of propagation of the output beams is normal to the OCM [17] in configuration 1, which causes the divergence angle to be smaller than that in configuration 2. In addition, the lower NA of the Er^{3+} - Yb^{3+} codoped double-clad fiber also makes it easier to achieve laser output with good beam quality. Furthermore, with relatively simple modifications to the cavity design (with a shorter focal-length collimating lens or a diffraction grating with a larger pitch), it should be possible to improve the beam quality M^2 to <1.1 [18–21].

4. Conclusion

In this study, according to the principle of laser generation, we simplify the two external cavity tunable systems into a fiber laser system. Based on the rate equation of Er/Yb codoped fiber laser and the established boundary conditions, the changes of the output powers with the wavelength were analyzed. The result shows that assuming the pump power is 2 W, the maximum tuning power of configuration 1 is 800 mW at 1545 nm. The maximum tuning power of configuration 2 is 600 mW at 1555 nm. Furthermore, the experimental setups of two kinds of external cavity tunable fiber lasers were also built, and their differences in output effects of them were compared and analyzed. For configuration 1, the measured maximum output power is 501 mW with a maximum slope efficiency of 24%, the tuning range is 32 nm from 1532 to 1564 nm, and M^2 is kept in the range of 1.22–1.24; the suppression of the signal background caused by ASE was better than 46 dB. For configuration 2, the maximum output power is 409 mW with a slope efficiency of 18.3%, the tuning range is 40 nm from 1530 to 1570 nm, and M^2 is kept in the range of 1.31–1.33. The suppression of the signal background caused by ASE was better than 41 dB. The backend feedback (R_3) of the resonator has a great influence

on the tunable range and output power. This research can provide potential value for the DWDM and fiber sensing system.

Data Availability

The (DATA TYPE) data used to support the findings of this study are included within the article.

Conflicts of Interest

The authors declare that they have no conflicts of interest.

Acknowledgments

This work was supported by the National Natural Science Foundation of China (41805014) and Natural Science Foundation of Anhui Province, China (1808085MF189, gxbjZD2021063, KJ2019A0565, and KJ2019A0576).

References

- [1] S. Zhan, Z. Wu, F. He, J. Zhang, J. C. You, and Y. W. Ma, "Influence of transform-lens focal length on spectral beam combining in an external cavity with a microlens array," *Optics Communications*, vol. 387, pp. 223–229, 2017.
- [2] X. Liu, S. Qiao, and Y. Ma, "Highly sensitive methane detection based on light-induced thermoelastic spectroscopy with a 2.33 μm diode laser and adaptive Savitzky-Golay filtering," *Optics Express*, vol. 30, no. 2, pp. 1304–1313, 2022.
- [3] N. Pavel, T. Dascalu, G. Salamu, M. Dinca, N. Boicea, and A. Birtas, "Ignition of an automobile engine by high-peak power Nd: YAG/Cr⁴⁺:YAG laser-spark devices," *Optics Express*, vol. 23, no. 26, Article ID 33028, 2015.
- [4] S. C. Zhao, P. Qin, D. Y. Yan et al., "Stable mode-locked Yb-fiber laser with a 6 MHz repetition rate tuning rang," *Infrared and Laser Engineering*, vol. 50, no. 3, Article ID 20200205, 2021.
- [5] S. L. Liu, Y. G. Li, Y. L. Gao, L. Ding, and K. C. Lu, "High-power widely tunable Yb-doped photonic crystal fiber laser," *Acta Optica Sinica*, vol. 27, no. 9, pp. 1663–1667, 2007.
- [6] J. Nilsson, W. A. Clarkson, R. Selvas et al., "High-power wavelength-tunable cladding-pumped rare-earth-doped silica fiber lasers," *Optical Fiber Technology*, vol. 10, no. 1, pp. 5–30, 2004.
- [7] Z. L. Wu, S. H. Zhao, X. C. Chu, L. Li, and S. B. Zhan, "Tunable Er³⁺-Yb³⁺ co-doped fiber laser based on blazed grating," *Chinese Journal of Lasers*, vol. 36, no. 6, pp. 1352–1355, 2009.
- [8] M. Auerbach, D. Wandt, C. Fallnich, H. Welling, and S. Unger, "High-power tunable narrow line width ytterbium-doped double-clad fiber laser," *Optics Communications*, vol. 195, no. 5-6, pp. 437–441, 2001.
- [9] Y. Zhang, Q. Zhao, C. Li et al., "Ultra-narrow linewidth full C-band tunable single-frequency linear-polarization fiber laser," *Optics Express*, vol. 23, Article ID 26214, 2016.
- [10] U. Wang, X. Zhu, R. A. Norwood, and N. Peyghambarian, "Widely wavelength tunable Dy³⁺/Er³⁺ co-doped ZBLAN fiber lasers," *Optics Express*, vol. 23, Article ID 38653, 2021.
- [11] S. M. Zhang, F. Y. Lu, X. Yang, F.-J. Dong, H.-J. Wang, and X. Dong, "Wavelength tunable linear cavity cladding pump Er³⁺/Yb³⁺ co-doped fiber laser operating in L-band," *Optical and Quantum Electronics*, vol. 37, no. 4, pp. 417–424, 2005.
- [12] S.-B. Zhan, Z.-L. Wu, J.-B. Hu et al., "Investigation on ultimate efficiency of spectral beam combining based on an external cavity," *Optik*, vol. 158, pp. 1519–1532, 2018.
- [13] E. J. Bochove, "Theory of spectral beam combining of fiber lasers," *IEEE Journal of Quantum Electronics*, vol. 38, pp. 432–445, 2002.
- [14] M. Laroche, S. Girard, J. K. Sahu, W. A. Clarkson, and J. Nilsson, "Accurate efficiency evaluation of energy-transfer processes in phosphosilicate Er³⁺-Yb³⁺-codoped fibers," *Journal of the Optical Society of America B*, vol. 23, 2006.
- [15] E. Yahel and A. Hardy, "Efficiency optimization of high-power Er³⁺-Yb³⁺-codoped fiber amplifiers for wavelength-division-multiplexing application," *Journal of the Optical Society of America B*, vol. 20, no. 6, pp. 1189–1197, 2003.
- [16] E. Yahel and A. Hardy, "Amplified spontaneous emission in high-power Er³⁺-Yb³⁺-codoped fiber amplifiers for wavelength-division-multiplexing application," *Journal of the Optical Society of America B*, vol. 20, no. 6, pp. 1198–1202, 2003.
- [17] Z. Wu, T. Ito, H. Akiyama, and B. Zhang, "Effect of interaction between the internal cavity and external cavity on beam properties in a spectrally beam combined system," *Journal of the Optical Society of America A*, vol. 35, no. 5, pp. 772–778, 2018.
- [18] N. A. Naderi, A. Flores, B. M. Anderson, and I. Dajani, "Beam combinable, kilowatt, all-fiber amplifier based on phase-modulated laser gain competition," *Optics Letters*, vol. 41, no. 17, pp. 3964–3967, 2016.
- [19] D. R. Drachenberg, O. Andrusyak, G. Venus, V. Smirnov, and L. B. Glebov, "Thermal tuning of volume Bragg gratings for spectral beam combining of high-power fiber lasers," *Applied Optics*, vol. 53, no. 6, pp. 1242–1246, 2014.
- [20] E. Honea, R. S. Afzal, M. Savage-Leuchs et al., "Advances in fiber laser spectral beam combining for power scaling," *Proceedings of SPIE*, vol. 9730, 2016.
- [21] E. J. Bochove, "Spectral beam combining of fiber lasers: tolerances, lens design, and microlens array inclusion," *Proceedings of SPIE*, vol. 4629, pp. 31–38, 2002.